The Arabidopsis Cyclic Nucleotide-Gated Ion Channels AtCNGC2 and AtCNGC4 Work in the Same Signaling Pathway to Regulate Pathogen Defense and Floral Transition[1][C][W][OPEN]

Kimberley Chin, Thomas A. DeFalco, Wolfgang Moeder, and Keiko Yoshioka*

Department of Cell and Systems Biology, University of Toronto, Toronto, Ontario, Canada M5S 3B2

Arabidopsis (*Arabidopsis thaliana*) cyclic nucleotide-gated ion channels (CNGCs) form a large family consisting of 20 members and have been implicated in Ca^{2+} signaling related to various physiological processes, such as pathogen defense, development, and thermotolerance. The null mutant of *AtCNGC2*, *defense, no death* (*dnd1*), exhibits autoimmune phenotypes, while it is impaired in mounting the hypersensitive response, which is a hallmark of effector-triggered (i.e. *RESISTANCE*-gene mediated) resistance. It has been suggested that *AtCNGC2* is involved in defense responses and likely other aspects of physiology through its role as a Ca^{2+}-conducting channel. However, the downstream signaling components and its relation with *AtCNGC4*, which is the closest paralog of *AtCNGC2*, remain elusive. Despite the fact that *cngc4* mutants display almost identical phenotypes to those seen in *cngc2* mutants, not much is known about their relationship. Here, we report the identification and characterization of the Arabidopsis mutant *repressor of defense no death1* (*rdd1*), obtained from a suppressor screen of a transfer DNA insertion knockout mutant of *AtCNGC2* in order to identify downstream components of *dnd1*-mediated signal transduction. *rdd1* suppressed the majority of *dnd1*-mediated phenotypes except Ca^{2+} hypersensitivity. In addition, *rdd1* also suppressed the *dnd1*-mediated late-flowering phenotype that was discovered in this study. Our genetic analysis conducted to elucidate the relationship between AtCNGC2 and AtCNGC4 indicates that *RDD1* is also involved in *AtCNGC4*-mediated signal transduction. Lastly, bimolecular fluorescence complementation analysis suggests that AtCNGC2 and AtCNGC4 are likely part of the same channel complex.

The Arabidopsis (*Arabidopsis thaliana*) *defense, no death* (*dnd1*) mutant is a rare autoimmune mutant that was identified by its reduced ability to produce a hypersensitive response (HR; Yu et al., 1998; Clough et al., 2000). The HR is a characteristic feature of effector-triggered (i.e. *RESISTANCE* [*R*]-gene mediated) resistance by which plants undergoing an attack by an avirulent pathogen induce a type of programmed cell death around the sites of pathogen entry (Hammond-Kosack and Jones, 1996; Greenberg and Yao, 2004). Despite the impairment of HR, the *dnd1* mutant displays typical autoimmune phenotypes, such as constitutive expression of *PATHOGENESIS-RELATED* (*PR*) genes, elevated levels of salicylic acid (SA), an important signaling molecule for pathogen resistance, and conditional HR-like spontaneous lesions without pathogen infection. Consequently, *dnd1* plants show enhanced broad-spectrum resistance against several taxonomically unrelated pathogens (Yu et al., 1998; Clough et al., 2000; Genger et al., 2008). The mutation in *dnd1* has been revealed to be a premature stop codon in the Arabidopsis cyclic nucleotide-gated ion channel (CNGC), *AtCNGC2*, and thus is a loss-of-function mutant of this gene (Clough et al., 2000).

CNGCs are nonselective cation channels that were first identified in vertebrate photoreceptors and olfactory sensory neurons (Zagotta and Siegelbaum, 1996; Craven and Zagotta, 2006). In animals, the biological roles of CNGCs and their regulation have been well studied, and CNGC subunits have been shown to form tetrameric channels at the plasma membrane that are directly regulated by cyclic nucleotides and the Ca^{2+} sensor protein, calmodulin (Kaupp and Seifert, 2002). On the other hand, plant CNGCs have only been investigated much more recently, and the mechanisms by which they are regulated are just starting to be revealed (Chin et al., 2009; Moeder et al., 2011).

Based on the Arabidopsis genome sequence, there are 20 members in the Arabidopsis CNGC family that are classified into four groups (groups I–IV), where group IV is further divided into subgroups IVA and IVB (Mäser et al., 2001). *AtCNGC2* belongs to group

[1] This work was supported by a Discovery Grant from the Natural Science and Engineering Research Council of Canada, the Canadian Foundation for Innovation, the Ontario Research Fund to K.Y., by graduate student fellowships from the Ontario government to K.C., and from the Natural Science and Engineering Research Council of Canada to T.A.D.

* Address correspondence to keiko.yoshioka@utoronto.ca.

The author responsible for distribution of materials integral to the findings presented in this article in accordance with the policy described in the Instructions for Authors (www.plantphysiol.org) is: Keiko Yoshioka (keiko.yoshioka@utoronto.ca).

[C] Some figures in this article are displayed in color online but in black and white in the print edition.

[W] The online version of this article contains Web-only data.

[OPEN] Articles can be viewed online without a subscription.

www.plantphysiol.org/cgi/doi/10.1104/pp.113.225680

IVB, together with only *AtCNGC4*. They are closely related to each other and distinctly different from the rest of the CNGC family members. Interestingly, loss-of-function mutants of *AtCNGC4*, *dnd2/hlm1*, show remarkably similar autoimmune phenotypes to *dnd1*, including an alteration of HR after avirulent pathogen infection (Balagué et al., 2003; Jurkowski et al., 2004). Thus, this observation raises the question of whether these two closely related CNGCs share the same biological function by a similar molecular mechanism.

Experiments in heterologous expression systems suggested that AtCNGC2 can form ion channels that conduct both Ca^{2+} and K^+ (Leng et al., 1999, 2002), although it has been mostly implicated in Ca^{2+} signaling (Ali et al., 2007; Urquhart et al., 2007; Finka et al., 2012). Furthermore, *dnd1* shows hypersensitivity to elevated Ca^{2+}, exhibiting severe growth suppression in medium containing 20 mM $CaCl_2$ (Chan et al., 2003). Genome-wide transcriptome analysis revealed that *dnd1* displays a similar transcriptional profile to that of wild-type plants grown in high-Ca^{2+} medium (Chan et al., 2008). It is known that Ca^{2+} influx and a rise in cytoplasmic Ca^{2+} play crucial roles in the signal transduction of defense responses and that pathogen recognition events can trigger a Ca^{2+} signal generated by plasma membrane-localized Ca^{2+}-conducting channels (McAinsh and Schroeder, 2009; Spalding and Harper, 2011). Using electrophysiology, AtCNGC2 was suggested to form such a channel that generates an inward Ca^{2+} current upon recognition of the bacterial elicitor lipopolysaccharide leading to nitric oxide generation (Ali et al., 2007). Thus, this also could be the case with AtCNGC4.

In addition to *AtCNGC2* and *AtCNGC4*, *AtCNGC11* and *AtCNGC12*, members of group I, are also postulated to be involved in plant immune responses. This was revealed in the study of the rare gain-of-function mutant *constitutive expresser of PR genes22 (cpr22)* that resulted from the fusion of *AtCNGC11* and *AtCNGC12* (Yoshioka et al., 2006). Similar to *dnd1* and *hlm1/dnd2*, *cpr22* displays autoimmune phenotypes with increased SA accumulation and constitutive *PR* gene expression. Additionally, *cpr22* mutants exhibit Ca^{2+}-dependent spontaneous cell death (Urquhart et al., 2007). However, unlike *dnd1* and *hlm1/dnd2*, they are able to induce an HR in response to avirulent pathogens (Yoshioka et al., 2006). Furthermore, *atcngc11* and *atcngc12* knockout mutants showed a partial breakdown of resistance against avirulent pathogens, indicating a striking difference in the molecular mechanisms that govern defense signaling mediated by *AtCNGC11* and *AtCNGC12* from that of *AtCNGC2* and *AtCNGC4* (Yoshioka et al., 2006; Moeder et al., 2011).

In order to better understand plant CNGC signal transduction, various epistatic analyses have been conducted with *dnd1*, *dnd2/hlm1*, and *cpr22*. These experiments revealed that mutations affecting the accumulation and/or perception of SA abolish enhanced resistance to the bacterial pathogen *Pseudomonas syringae* and the oomycete pathogen *Hyaloperonospora arabidopsidis* observed in *dnd1*, *hlm1/dnd2*, and *cpr22* (Clough et al., 2000; Yoshioka et al., 2001, 2006; Jurkowski et al., 2004; Genger et al., 2008). Therefore, despite the differences in HR responses, the enhanced resistance phenotype in these mutants was established to be SA dependent. Additionally, *PHYTOALEXIN DEFICIENT4*, *ENHANCED DISEASE SUSCEPTIBILITY1*, and *NON-RACE-SPECIFIC DISEASE RESISTANCE1* are important components of the resistance regulated by the aforementioned CNGCs (Jirage et al., 2001; Yoshioka et al., 2001, 2006; Genger et al., 2008). Alterations in jasmonic acid (JA) and ethylene (ET) signaling pathways, which mediate wounding, herbivory, and the resistance response to nectrotrophic pathogen attack, have also been observed in these mutants (Yoshioka et al., 2001; Jurkowski et al., 2004; Genger et al., 2008). Along with *PR* genes, *cpr22* constitutively expresses the JA-inducible antifungal defensin gene *PDF1.2*, which is suppressed when crossed to mutants of JA/ET signaling, thereby indicating that the mutation not only activates SA-dependent signaling pathways but JA/ET-dependent ones as well (Yoshioka et al., 2001). In contrast, *PDF1.2* is not expressed in *dnd1*, but it is highly induced when SA-associated pathways are impaired (Jirage et al., 2001; Genger et al., 2008). However, the mechanism by which this redirection of both signaling pathways occurs remains unknown. Thus, there is increasing evidence that implicates CNGCs in regulating pathogen defense responses through separate but partially overlapping pathways. Many of the signaling components in these pathways, however, still remain to be elucidated despite significant progress.

Here, we report the identification and characterization of the Arabidopsis mutant *repressor of defense no death1* (*rdd1*), obtained from a suppressor screen of a transfer DNA (T-DNA) knockout mutant of *AtCNGC2* in order to identify downstream components of *dnd1*-mediated signal transduction. *rdd1* suppressed the majority of *dnd1*-mediated phenotypes except Ca^{2+} hypersensitivity. In addition, *rdd1* suppressed the *dnd1*-mediated floral transition phenotype that was discovered in this study. Our genetic analysis conducted to elucidate the relationship between *dnd1*-mediated and *hlm1/dnd2*-mediated resistance signaling pathways indicates that *RDD1* is also involved in *AtCNGC4*-mediated signal transduction. The data presented here provide evidence of the overlapping nature of the two signaling pathways and possible heterotetramerization of AtCNGC2 and AtCNGC4. Finally, bimolecular fluorescence complementation (BiFC) analysis in *Nicotiana benthamiana* suggests that AtCNGC2 and AtCNGC4 subunits form homotetrameric and heterotetrameric channels in planta.

RESULTS

Identification of *rdd1*

A T-DNA insertion homozygous line (Salk_066908) for *AtCNGC2* (At5g15410) was obtained from The

Arabidopsis Information Resource (www.arabidopsis.org; Supplemental Fig. S1A). We named this line *cngc2-3*. Homozygosity of the insertion was confirmed by PCR analysis, and the lack of expression of proper full-length mRNA was confirmed by reverse transcription-PCR (Supplemental Fig. S1B). As we expected, the morphological phenotype of this line is identical to the null mutant, *dnd1*, further confirming the functional knockout status of this mutant (Fig. 1A). Approximately 10,000 *cngc2-3* seeds were mutagenized with ethyl methanesulfonate and screened for plants suppressing the morphological phenotype of *cngc2* in the M2 generation. *rdd1* with the *cngc2-3* background, designated *rdd1 cngc2-3*, was identified based on its intermediate morphology between the Columbia (Col) wild type and *cngc2* (Fig. 1A). The *cngc2-3* background of *rdd1 cngc2-3* was confirmed by PCR analysis (Supplemental Fig. S1C). *dnd1* has been reported to exhibit conditional spontaneous lesion formation (Clough et al., 2000). Under our growth conditions, we observed this lesion formation in *dnd1* as well as *cngc2-3*, while this phenotype was suppressed in *rdd1 cngc2-3* (Fig. 1A). To determine the genetic nature, *rdd1 cngc2-3* plants were backcrossed to *cngc2-3* plants. All B1 (backcrossed, first generation) plants displayed *rdd1 cngc2-3* morphology, suggesting that *rdd1* is a dominant mutation (Table I). The subsequent self-pollinated B2 generation (backcrossed, selfed) segregated with a 3:1 (*rdd1 cngc2-3*:*cngc2-3*) phenotypic ratio, indicating that the morphological phenotype of *rdd1 cngc2-3* segregates as a single locus that is dominant to the wild-type *RDD1* allele (Table I). Thus, hereafter, we call this mutant *rdd1-1D cngc2-3*.

rdd1-1D cngc2-3 Suppresses the HR-Deficient Phenotype in *cngc2* (*dnd1*) Mutants

The partial suppression of the *cngc2*-conferred dwarfism in *rdd1-1D cngc2-3* prompted us to assess other *dnd1*-related phenotypes. As mentioned above, *dnd1* plants display reduced or absent HR upon infection with avirulent pathogens. To examine the effect of the *rdd1-1D* mutation on HR formation, *rdd1-1D cngc2-3* leaves were inoculated with avirulent *P. syringae* pv *glycinea* expressing *avrRpt2* (*Psg avrRpt2*$^+$) and assessed for HR induction. At 24 h post inoculation, Col wild-type leaves displayed HR as visible leaf collapse, which was absent in *rdd1-1D cngc2-3*, *cngc2-3*, and *dnd1* leaves (Fig. 1B). Plant cells that undergo HR display significant increases in autofluorescence due to the production of phenolic compounds (Yu et al., 1998). Therefore, to closely monitor HR induction, leaf discs were excised from the inoculated areas and viewed with a microscope to compare HR-induced autofluorescence. As seen in Figure 1C, Col wild-type inoculated leaves exhibited a high level of autofluorescence. Interestingly, a marked increase in autofluorescence was also observed in *rdd1-1D cngc2-3* inoculated leaves compared with *cngc2-3* and *dnd1*, although to a lesser degree than

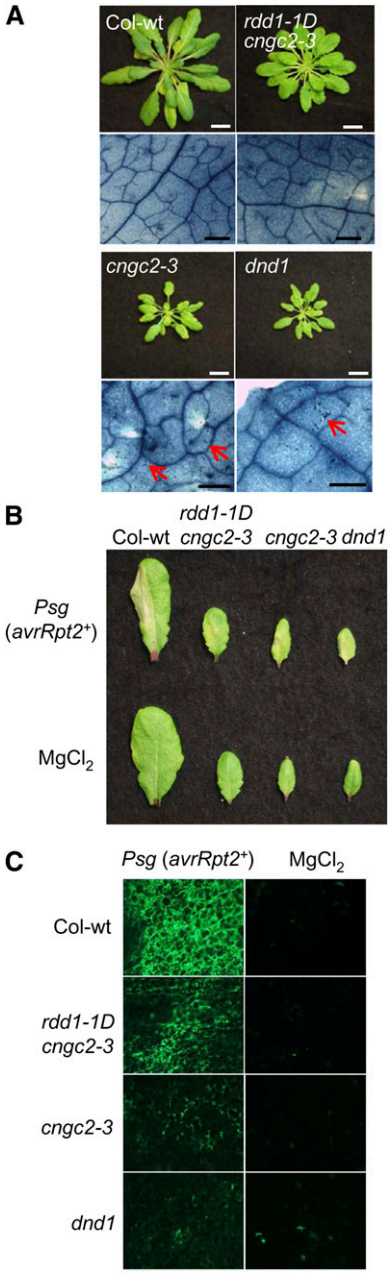

Figure 1. *rdd1-1D* suppresses *cngc2*-conferred phenotypes. A, Morphological phenotype of 5-week-old Col wild-type (Col-wt), *rdd1-1D cngc2-3*, *cngc2-3*, and *dnd1* plants. *cngc2-3* mutants are stunted in growth and exhibit conditional lesion formation identical to *dnd1*. *rdd1-1D cngc2-3* plants display intermediate rosette morphology between the wild type and *cngc2-3*. White bars = 1 cm. Trypan blue staining reveals the reduction of cell death in *rdd1-1D cngc2-3* compared with *cngc2-3*. Red arrows indicate cell death. Black bars = 50 μm. B, Macroscopic cell death (HR) upon infection with *Psg avrRpt2*$^+$ Col wild-type leaves exhibited visible HR at 24 h, while *rdd1-1D cngc2-3*, *cngc2-3*, and *dnd1* did not. $MgCl_2$ infiltrations served as negative controls. C, Microscopic cell death was monitored using fluorescence microscopy. Inoculated wild-type leaves displayed significant autofluorescence compared to *cngc2-3* and *dnd1*. *rdd1-1D cngc2-3* leaves also displayed autofluorescence, but to a lesser extent than the Col wild type. $MgCl_2$ infiltrations served as negative controls. [See online article for color version of this figure.]

Table I. *Segregation analysis of the rdd1-1D cngc2-3 phenotype*

Plant Line	Backcross	Total No.	Morphological Phenotype		Hypothesis	χ^{2a}	*P*
			rdd1-1D cngc2-3	*cngc2-3*			
rdd1-1D/RDD1 selfed		112	92	20	3:1	3.04	$0.95 > P > 0.9$
rdd1-1D cngc2-3 × *cngc2-3*	B1[b]	13	13	0	1:0		
	B2[c]	105	77	28	3:1	0.16	$0.95 > P > 0.9$

[a]One degree of freedom. [b]Backcross of the first generation of *rdd1* and *cngc2-3* plants. [c]Backcross of the second generation of selfed B1 plants.

the Col wild type (Fig. 1C). Similar results were also observed in plants inoculated with *P. syringae* pv *tomato* expressing *avrRpt2* (data not shown). Taken together, the mutation partially suppresses the HR-deficient phenotype observed in *cngc2-3* and *dnd1* plants in response to avirulent pathogen infection.

rdd1-1D cngc2-3 Partially Loses *cngc2*-Conferred Autoimmune Phenotypes

As mentioned previously, *cngc2* mutant plants display autoimmune phenotypes, such as elevated levels of SA and constitutive expression of *PR* genes. They also display enhanced resistance to virulent strains of *P. syringae* and *H. arabidopsidis* despite their HR-deficient phenotypes. To examine the effect of the *rdd1-1D* mutation on these phenotypes, the growth of the bacterial pathogen *P. syringae* pv *tomato* DC3000 was measured. As shown in Figure 2A, both *dnd1* and *cngc2-3* showed reduced pathogen growth compared with the Col wild type, whereas *rdd1-1D cngc2-3* did not. A similar breakdown of *cngc2*-conferred enhanced resistance was also observed after infection with the virulent oomycete pathogen *H. arabidopsidis*, isolate Noco2. This strain is virulent to the Col ecotype, which is the background of both *dnd1* and *cngc2-3*. As shown in Figure 2B, a partial breakdown of enhanced resistance in *cngc2* was observed in *rdd1-1D cngc2-3*. As reported previously, *dnd1* plants display autoinduction of *PR-1* gene expression. This was also observed in *cngc2-3*. However, it was significantly reduced in *rdd1-1D cngc2-3* (Fig. 2C). These data indicate a reduction of *cngc2*-mediated accumulation of SA in *rdd1-1D cngc2-3*; thus, the endogenous level of total SA was measured. Similar to *PR-1* gene expression, lower levels of total SA in *rdd1-1D cngc2-3* compared with *dnd1* and *cngc2-3* were detected (Fig. 2D). Taken together, the *rdd1-1D* mutation suppressed the autoimmune phenotype conferred by *cngc2*.

cngc2 Affects the Floral Transition, and the *rdd1-1D* Mutation Suppresses This Novel *dnd1*-Conferred Phenotype

Through characterization of *rdd1-1D cngc2-3*, we discovered a novel phenotype in *cngc2/dnd1*. Under our long-day (16 h of light/8 h of dark) and ambient humidity conditions, Col wild-type plants flowered 23 d post stratification, while *cngc2-3* and *dnd1* mutant plants flowered significantly later, at 29 d post stratification (Fig. 3, A and B). This novel phenotype was also repressed in *rdd1-1D cngc2-3* plants, which flowered at approximately the same time as the Col wild type (Fig. 3B). Delayed flowering can also be reflected by an increased number of rosette leaves prior to bolting. As shown in Figure 3C, Col wild-type plants had significantly fewer rosette leaves at the time of flowering compared with *cngc2-3* and *dnd1* plants, confirming the delayed-flowering phenotype of *cngc2* and *dnd1* mutants. Similar to the Col wild type, the rosette leaf number in *rdd1-1D cngc2-3* was significantly reduced compared with *cngc2-3* and *dnd1* (Fig. 3C), indicating that the mutation in *RDD1* suppresses the delayed floral transition observed in *cngc2* mutants. Similar but more pronounced results were observed under short days (8 h of light/16 h of dark; Supplemental Table S1). Consistent with these results, expression levels of the floral repressor *FLOWERING LOCUS C* (*FLC*; He and Amasino, 2005) were significantly elevated in *cngc2-3* and *dnd1* compared with the Col wild type, while wild-type expression levels were observed in *rdd1-1D cngc2-3* (Fig. 3D). Taken together, a novel delayed-flowering phenotype was observed in *cngc2* and *dnd1* mutants, which is likely caused by an alteration in *FLC* expression. This phenotype was abolished in *rdd1-1D cngc2-3* under both long- and short-day conditions.

The *rdd1-1D* Mutation Does Not Rescue the Ca^{2+} Hypersensitivity of *cngc2* Mutants

It was previously shown that null mutations of *AtCNGC2* lead to hypersensitivity to Ca^{2+} that impairs plant growth (Chan et al., 2003). To determine whether *rdd-1D* also suppresses this phenotype, we compared the size of Col wild-type, *rdd1-1D cngc2-3*, *cngc2-3*, and *dnd1* plants grown in Ca^{2+}-supplemented medium. As seen in Figure 4A, although slight chlorosis was observed, Col wild-type plants did not display any strong suppression in growth with 20 mM Ca^{2+}-supplemented medium. In contrast, *cngc2-3* and *dnd1* plants exhibited severely stunted growth and chlorosis, which was consistent with the previous report (Chan et al., 2003). Unexpectedly, *rdd1-1D cngc2-3* plants also displayed stunted growth and severe chlorosis similar to *cngc2-3* and *dnd1*, indicating that *rdd1-1D* does not suppress

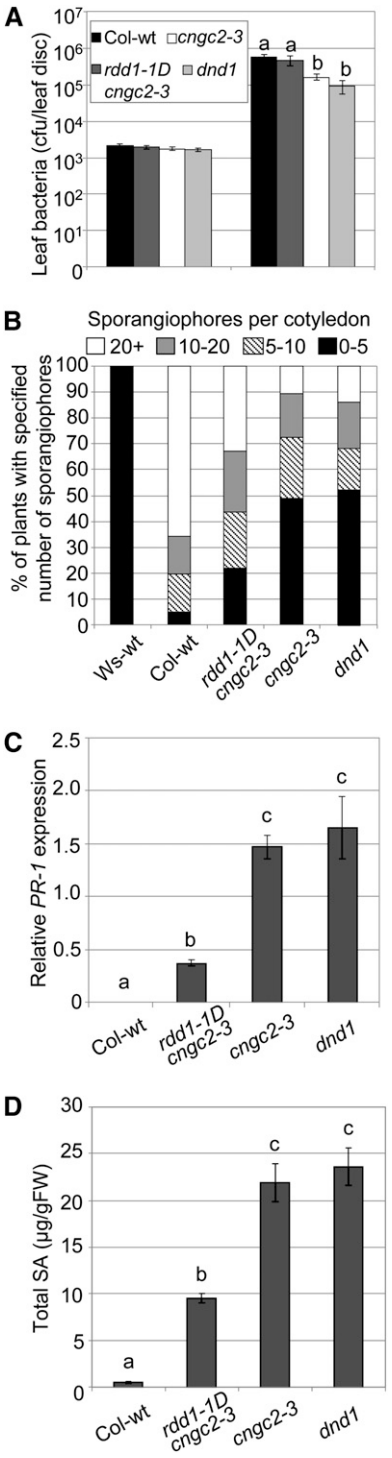

Figure 2. *rdd1-1D* partially suppresses the *cngc2*-mediated constitutive defense response. A, Leaf bacterial populations were assessed 3 d after infiltration with virulent *P. syringae* pv *tomato* DC3000 at 5×10^4 colony-forming units (cfu) mL^{-1}. Col wild-type (Col-wt) and *rdd1-1D cngc2-3* leaves supported significantly more bacterial growth compared with *cngc2-3* and *dnd1*. Bars marked with different letters indicate significant differences (Student's *t* test, $P < 0.05$). Data are representative of seven experiments. B, Col wild-type, Wassilewskija wild-type (Ws-wt), and mutant cotyledons ($n = 40$) were inoculated with *H. arabidopsidis*, isolate Noco2, at a suspension of 8×10^5 spores mL^{-1} and monitored for sporangiophore formation. At 7 d post inoculation, *rdd1-1D cngc2-3* cotyledons supported an intermediate level of sporangiophore formation between the Col wild type and *cngc2-3*. The Wassilewskija ecotype is resistant to Noco2 and served as a control. Data are representative of two separate experiments. C, *PR-1* transcript levels in 3- to 4-week-old Col wild-type and mutant leaves measured by qRT-PCR. *PR-1* expression is shown relative to *EF-1α*. Error bars indicate SE of three replicates. Bars marked with different letters indicate significant differences (Student's *t* test, $P < 0.05$). D, Total SA levels (SA + SA-glucoside) in 3- to 4-week-old wild-type and mutant leaves. Error bars indicate SE of three replicates. Bars marked with different letters indicate significant differences (Student's *t* test, $P < 0.05$). FW, Fresh weight.

Ca^{2+} hypersensitivity of *cngc2*. This observation was also confirmed quantitatively by measuring the average fresh weight of each genotype. As shown in Figure 4B, *rdd1-1D cngc2-3*, *cngc2-3*, and *dnd1* plants showed significant size reductions compared with the Col wild type on medium supplemented with 20 mM Ca^{2+}. To assess whether the suppression is partial, lower concentrations of Ca^{2+} (5 and 10 mM) were also tested. As shown in Supplemental Figure S2, there was no statistical significance in these lower concentrations between *rdd1-1D cngc2-3* and *cngc2-3*. Taken together, the mutation of *rdd1* does not suppress the Ca^{2+} hypersensitivity of *cngc2* mutants.

RDD1 Is Involved in Both CNGC2- and CNGC4-Mediated Signal Transduction

It has been reported that null mutants of *AtCNGC4* (*hlm1/dnd2*) exhibit strikingly similar phenotypes to *cngc2-3* and *dnd1* plants, such as dwarfism, enhanced pathogen resistance, and an impaired HR response to avirulent pathogens (Balagué et al., 2003; Jurkowski et al., 2004). As mentioned, AtCNGC2 and AtCNGC4 are the sole members of group IVB and share high sequence similarity (Mäser et al., 2001). This prompted us to investigate whether *rdd1* can also suppress *dnd2*-mediated phenotypes. For this analysis, we used an *AtCNGC4* T-DNA insertion line (Salk_081369). The homozygosity of the T-DNA insertion as well as the knockout status of this line (i.e. expression) were confirmed by PCR analysis and reverse transcription-PCR, respectively, and this line was named *cngc4-5* (Supplemental Figs. S1, A and B, and S3A). We crossed this line with *rdd1-1D cngc2-3* plants. All F1 plants were genotyped to confirm the existence of the T-DNA insertion in *AtCNGC2* and *AtCNGC4* (data not shown). Following self-pollination, a total of 243 F2 plants were monitored for their morphological phenotypes. As shown in Table II, they segregated in a 148:78:15:2 (wild type:*rdd1-1D cngc2-3*-like:*dnd*-like:enhanced *dnd* phenotype [termed *superdnd*]; Supplemental Fig. S3) ratio. This observation fits the expected ratio of 36:21:6:1, which was predicted in the case that *rdd1* suppresses not only *cngc2*-conferred, but also *cngc4*-conferred, phenotypes and even the *cngc2*

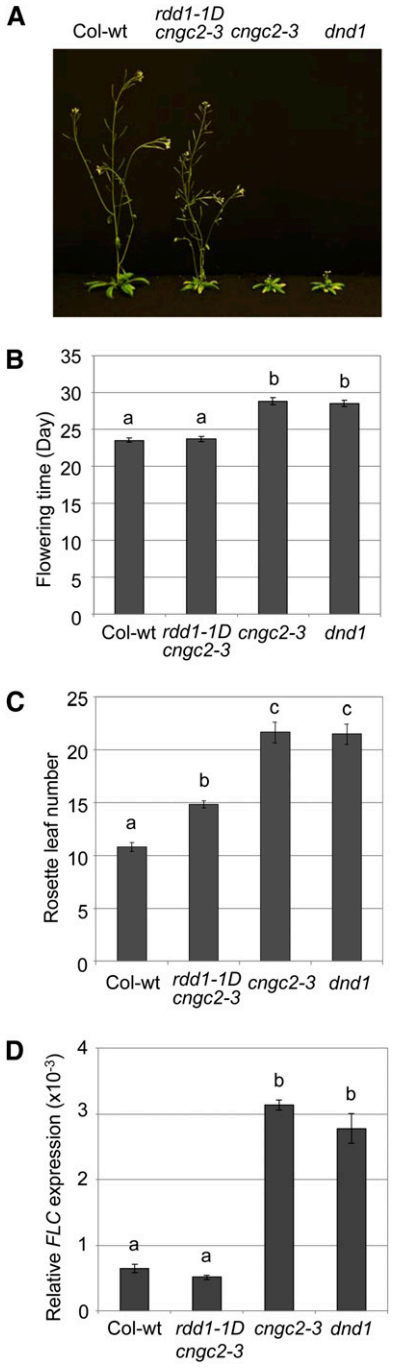

Figure 3. *rdd1-1D* represses the *cngc2*-mediated delay in floral transition. A, *cngc2-3* and *dnd1* plants exhibit delayed flowering compared with the Col wild type (Col-wt) and *rdd1-1D cngc2-3*. B, Flowering time was measured in Col wild-type and mutant plants by determining the emergence of the first bud. Data are representative of a total of four experiments. Error bars indicate SE of the average flowering time of approximately 30 to 40 plants. Bars marked with different letters indicate significant differences (Student's *t* test, $P < 0.05$). C, Rosette leaf number was measured upon bolting. Values represent means of 30 to 40 plants. Error bars indicate SE, and bars marked with different letters indicate significant differences (Student's *t* test, $P < 0.05$). D, qRT-PCR analysis of *FLC* expression. The expression is shown relative to *EF-1α*. Error bars indicate SE of three replicates. Bars marked with different letters indicate significant differences (Student's *t* test, $P < 0.05$). [See online article for color version of this figure.]

cncg4 double mutation, which has been reported to enhance the *dnd* phenotype (Table II; Supplemental Fig. S3; Jurkowski et al., 2004). In addition, the data suggest that the single *rdd1-1D* mutation does not cause a significant morphological difference compared with the Col wild type. This was confirmed by the phenotypes of F1 plants generated from a cross between *rdd1-1D cngc2-3* and the Col wild type (Supplemental Fig. S4).

The T-DNA insertion status in all 78 individuals exhibiting *rdd1-1D cngc2-3*-like morphology was analyzed, and the repression of the *cngc4* mutant as well as *cngc2 cncg4* double mutant phenotypes by *rdd1-1D* were confirmed (Supplemental Fig. S3). Taken together, the data indicate that the *rdd1-1D* mutation also suppresses *cngc4* (*hlm1/dnd2*)-conferred morphological phenotypes to the same degree as *cngc2*-conferred phenotypes.

The *rdd1-1D* Mutation Suppresses *cngc4*-Mediated Autoimmune Phenotypes

To assess the effect of *rdd1-1D* on *dnd2/cngc4*, we isolated *rdd1-1D cngc4-5* double mutants (Supplemental Fig. S3)from the above F2 plants. The *rdd1-1D cngc4-5* double mutant displayed the same phenotype *as rdd1-1D*

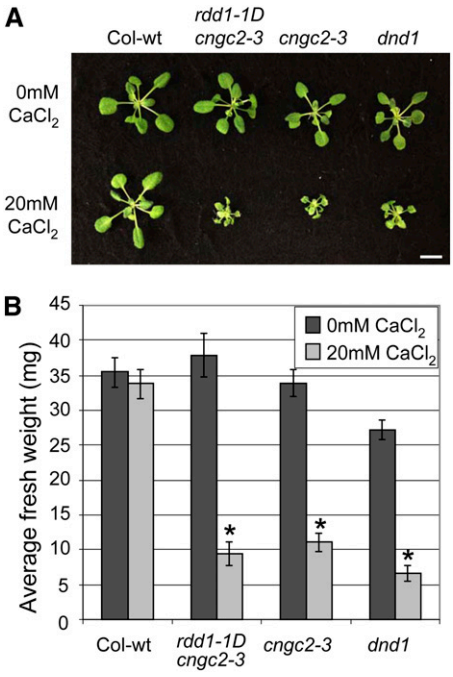

Figure 4. *rdd1-1D* does not rescue Ca^{2+} hypersensitivity in *cngc2*. A, Col wild-type (Col-wt) and mutant plants grown on both control medium and medium supplemented with 20 mM $CaCl_2$. At 3 weeks, *rdd1-1D cngc2-3*, *cngc2-3*, and *dnd1* plants are indistinguishable from the Col wild type when grown on control medium but exhibit severely stunted growth and chlorosis on 20 mM $CaCl_2$. Bar = 1 cm. B, Average fresh weights of 3-week-old Col wild-type and mutant plants grown on control medium and medium supplemented with 20 mM $CaCl_2$. Error bars indicate SE of four replicate plates (20 plants per plate). Asterisks indicate significant differences between 0 and 20 mM $CaCl_2$. (Student's *t* test, $P < 0.05$). [See online article for color version of this figure.]

Table II. *Segregation analysis of rdd1-1D cngc2-3 and cngc4-5 cross progeny*

Cross[a]	Generation	Total No.	Morphological Phenotype				Hypothesis[b]	χ^{2c}	*P*
			Wild Type	*rdd1-1D cngc2-3*	*dnd*	*superdnd*			
rdd1-1D cngc2-3 × *cngc4-5/cngc4-5*	F2	243	148	78	15	2	36:21:6:1	4.49	$0.95 > P > 0.9$

[a]The pollen acceptor plant is indicated first, and the pollen donor is second. [b]Hypothesis: *rdd1-1D* is inherited as a dominant mutation. *rdd1-1D* (dominant), *cngc2* (recessive), and *cngc4* (recessive) mutations segregate independently in the F2 generation. Suppression of *cngc4* by *rdd1-1D* results in a higher ratio of *rdd1-1D cngc2-3*-like to *dnd*-like plants (36:21:6:1, wild type:*rdd1*:*dnd*:*superdnd*). In contrast, no suppression by *rdd1-1D* results in a higher ratio of *dnd*-like to *rdd1*-like plants (36:9:18:1, wild type:*rdd1*:*dnd*:*superdnd*). The latter hypothesis was rejected ($\chi^2 = 99.48$). [c]Three degrees of freedom.

cngc2-3 (Fig. 5A), suggesting that the *rdd1-1D* mutation also suppresses *cngc4* phenotypes. To examine the effect of the mutation on *cngc4* (*hlm1/dnd2*)-conferred autoimmune phenotypes, we first monitored HR induction upon infection with *Psg avrRpt2*$^+$ in *rdd1-1D cngc4-5* plants. At 24 h post inoculation, Col wild-type leaves displayed visible leaf collapse, whereas *rdd1-1D cngc4-5*, *cngc4-5*, and *dnd2* leaves did not (Fig. 5B). For further evaluation, HR-induced autofluorescence was monitored. Similar to *rdd1-1D cngc2-3*, *rdd1-1D cngc4-5* leaves displayed a marked increase in autofluorescence compared with *cngc4* and *dnd2*, suggesting that *rdd1-1D* also suppresses *cngc4*-mediated alteration in HR (Fig. 5C). Next, we tested for enhanced resistance against virulent *H. arabidopsidis*, isolate Noco2, on 10-d-old seedlings. At 7 d post inoculation, *rdd1-1D cngc4-5* showed a partial breakdown of enhanced resistance similar to *rdd1-1D cngc2-3* compared with *cngc2-3* and *cngc4-5* single mutants (Fig. 5D). As expected, quantitative real-time (qRT)-PCR results from 5-week-old leaves showed a marked decrease in *PR-1* gene expression in *rdd1-1D cngc4-5* compared with *cngc4* and *dnd2* mutants (Fig. 5E). Delayed flowering was also observed in *cngc4-5* and *dnd2*, and this phenotype was also suppressed in *rdd1-1D cngc4-5* (Supplemental Fig. S5). Taken together, *rdd1-1D* suppresses *cngc4*-conferred phenotypes to a similar degree to those of *cngc2*. These results demonstrate that *AtCNGC2* and *AtCNGC4* participate in the same signaling pathway in mediating immunity and the floral transition.

CNGC2 and CNGC4 Subunits Likely Interact in Planta

Animal CNGC subunits have been shown to form heterotetrameric channels at the plasma membrane, where they mediate ion fluxes into the cell. However, the composition of the CNGCs and subunit interactions in plants remain unknown (Moeder et al., 2011). Since the genetic analysis and characterization of *rdd1-1D cngc4-5* indicated that *RDD1* participates in signaling mediated by both *AtCNGC2* and *AtCNGC4*, two possible scenarios arise. One scenario is that AtCNGC2 and AtCNGC4 subunits form homomeric channels at the plasma membrane to regulate parallel pathways that converge downstream. In this case, the suppression effect by the *rdd1* mutation should occur after the convergence of the two pathways. Alternatively, AtCNGC2 and AtCNGC4 subunits might be partners that form heteromeric channels that regulate one pathway that is affected by the *rdd1* mutation. To examine the subunit interactions, FPLC combined with western blotting using recombinantly expressed C-terminal peptides of CNGC2 and CNGC4 was performed (Supplemental Materials and Methods S1). This analysis had previously been used to evaluate the homomeric interaction of the C terminus of CNGC11/12 (same as 12; Abdel-Hamid et al., 2013). As shown in Supplemental Figure S6, the elution of the C-terminal recombinant proteins resulted in two peaks. The first peak eluted much earlier than the predicted tetramer size (suggesting a mass of more than 200 kD), indicating multimerization or aggregation of peptides. In both cases, the first peak appeared to contain full-length recombinant proteins, while the second peak was eluted between 45 and 50 kD, corresponding to the size of the tags, glutathione *S*-transferase (25 kD, which forms a dimer in solution) and maltose-binding protein (45 kD), for CNGC2 and CNGC4, respectively. Fractions corresponding to these peaks were collected separately and subjected to SDS-PAGE followed by western blotting using anti-glutathione *S*-transferase or anti-maltose-binding protein antibodies. Signals were detected in both peaks, and the size of the band confirmed that the first peak contained multimers or aggregates of CNGC2 or CNGC4 peptides and the second peak contained truncated tags only (Supplemental Fig. S6).

In our previous work with CNGC12 (11/12), a similar multimer peak was observed, and site-directed mutagenesis confirmed the interaction of the subunits (Abdel-Hamid et al., 2013). Thus, the data here also indicate the possibility of an interaction of CNGC2 and CNGC4. However, we cannot rule out that CNGC2 and CNGC4 monomeric aggregates merely coelute in the first peak. Thus, to evaluate the subunit interaction further, BiFC was conducted with full-length CNGC2 and CNGC4 in planta. For this analysis, full-length AtCNGC2 and AtCNGC4 were fused C terminally to the N- and C-terminal portions of yellow fluorescent protein (YFP; YFP^N and YFP^C, respectively) and transiently coexpressed under the control of the constitutive cauliflower mosaic virus 35S promoter in *N. benthamiana* leaves by *Agrobacterium tumefaciens* infiltration. This method has been used to evaluate the in planta subunit interaction of plant CNGCs (Abdel-Hamid et al., 2013). At 48 h post infiltration, weak but reproducible fluorescence was detected with AtCNGC2-YFP^N + AtCNGC4-YFP^C

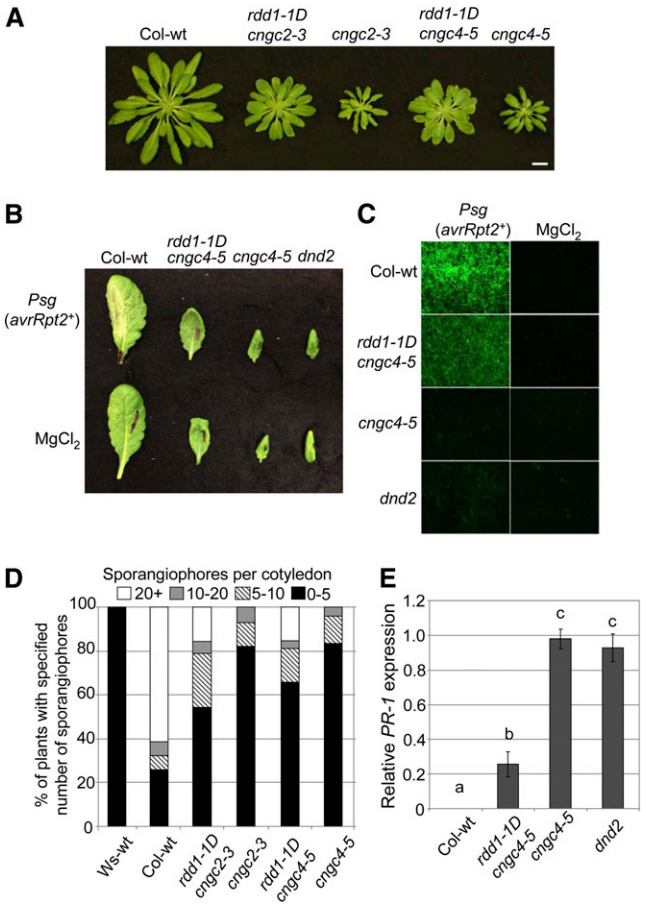

Figure 5. *rdd1* suppresses the *cngc4*-mediated autoimmune phenotypes. A, Morphological phenotype of 5-week-old Col wild-type (Col-wt), *rdd1-1D cngc2-3*, *cngc2-3*, *rdd1-1D cngc4-5*, and *cngc4-5* plants. *rdd1-1D cngc4-5* plants exhibit an intermediate rosette morphology similar to *rdd1-1D cngc2-3*. Bar = 1 cm. B, Col wild-type, *rdd1-1D cngc4-5*, *cngc4-5*, and *dnd2* leaves were infiltrated with avirulent *Psg avrRpt2*$^+$ at 2×10^8 colony-forming units mL^{-1} and assessed for HR. Col wild-type leaves exhibit visible HR at 24 h, while *rdd1/cngc4*, *cngc4-1*, and *dnd2* leaves did not. $MgCl_2$ infiltrations served as negative controls. C, *rdd1-1D cngc4-5* leaves displayed significant autofluorescence 24 h after infiltration with *Psg avrRpt2*$^+$, but to a lesser extent than the Col wild type. $MgCl_2$ infiltrations served as negative controls. D, Col wild-type and mutant cotyledons (n = 40) were inoculated with virulent *H. arabidopsidis*, isolate Noco2, at a suspension of 8×10^5 spores mL^{-1} and monitored for sporangiophore formation. At 7 d post inoculation, *rdd1-1D cngc4-5* cotyledons supported similar levels of sporangiophore formation as *rdd1-1D cngc2-3* and were less resistant than *cngc4-5*. E, *PR-1* transcript levels in 3- to 4-week-old Col wild-type and mutant leaves were measured by qRT-PCR. *PR-1* expression is shown relative to *EF-1α*. Error bars indicate SE of three replicates. Bars marked with different letters indicate significant differences (Student's t test, $P < 0.05$). [See online article for color version of this figure.]

coexpression, indicating that AtCNGC2 and AtCNGC4 subunits are able to form heteromeric channels (Fig. 6A). Reciprocal coexpression showed similar results (Fig. 6B). Interestingly, AtCNGC2-YFP^N + AtCNGC2-YFP^C and AtCNGC4-YFP^N + AtCNGC4-YFP^C combinations also produced weak but detectable fluorescence, indicating that AtCNGC2 and AtCNGC4 subunits are able to form homomeric channels (Fig. 6, C and D). YFP signals were not observed in single infiltrations of each construct (Fig. 6, E–H). Furthermore, coinfiltration of an unrelated subunit, AtCNGC11/12, with CNGC2 or CNGC4 did not show any signals, whereas AtCNGC11/12 can interact with itself (Yoshioka et al., 2006; Moeder et al., 2011; Abdel-Hamid et al., 2013, Supplemental Fig. S7, A–E). Since the expression of full-length YFP-tagged AtCNGC2, AtCNGC4, and AtCNGC11/12 was very comparable, the signal we observed with coexpressed CNGC2 and CNGC4 cannot be simply due to the overexpression by the cauliflower mosaic virus 35S promoter (Supplemental Fig. S7, F–H). We also note that it is almost impossible to visualize CNGC expression by fluorescent proteins using a weak promoter, since their expression is very low or unstable. In addition, the interaction with other unrelated proteins, such as transcription factors and kinases, was also tested. None of these control experiments showed BiFC signals (data not shown), confirming the specificity of the interaction between AtCNGC2 and AtCNGC4. Taken together, these results suggest the ability of AtCNGC2 and AtCNGC4 subunits to form both homomeric and heteromeric channels in planta.

DISCUSSION

Our understanding of the role of Ca^{2+}-based signaling in plants has significantly improved over the last 20 years, and it is now clear that Ca^{2+} plays crucial roles in the signal transduction by which a wide variety of abiotic, biotic, and developmental stimuli are transmitted (McAinsh and Schroeder, 2009). The influx of Ca^{2+} into the cytosol is accomplished by plasma membrane- and endomembrane-localized cation transport proteins. Genomic sequence data indicated that Arabidopsis contains over 150 cation transport proteins (Mäser et al., 2001). Among them, CNGCs were suggested to be involved in Ca^{2+} signaling. Arabidopsis CNGCs form a large gene family consisting of 20 members that have been implicated in a diverse range of biological phenomena, such as defense responses, gravitropism, pollen tube growth, ion homeostasis, and, very recently, thermotolerance (Talke et al., 2003; Frietsch et al., 2007; Kaplan et al., 2007; Chin et al., 2009; Urquhart et al., 2011; Finka et al., 2012; Tunc-Ozdemir et al., 2013).

CNGCs were first discovered in retinal photoreceptors and olfactory sensory neurons, and so far, six CNGC genes have been found in mammalian genomes (Zufall et al., 1994; Zagotta and Siegelbaum, 1996). Important functional features of CNGCs were studied extensively in animal systems, and it has been suggested that the subunit composition of the respective channel complex is an important determinant of functional features such as ligand sensitivity, selectivity, and gating (Kaupp and Seifert, 2002). For instance, native CNGCs in rod cells consist of two types of subunits, A1 and B1a. On the other hand, the CNGCs in the chemosensitive

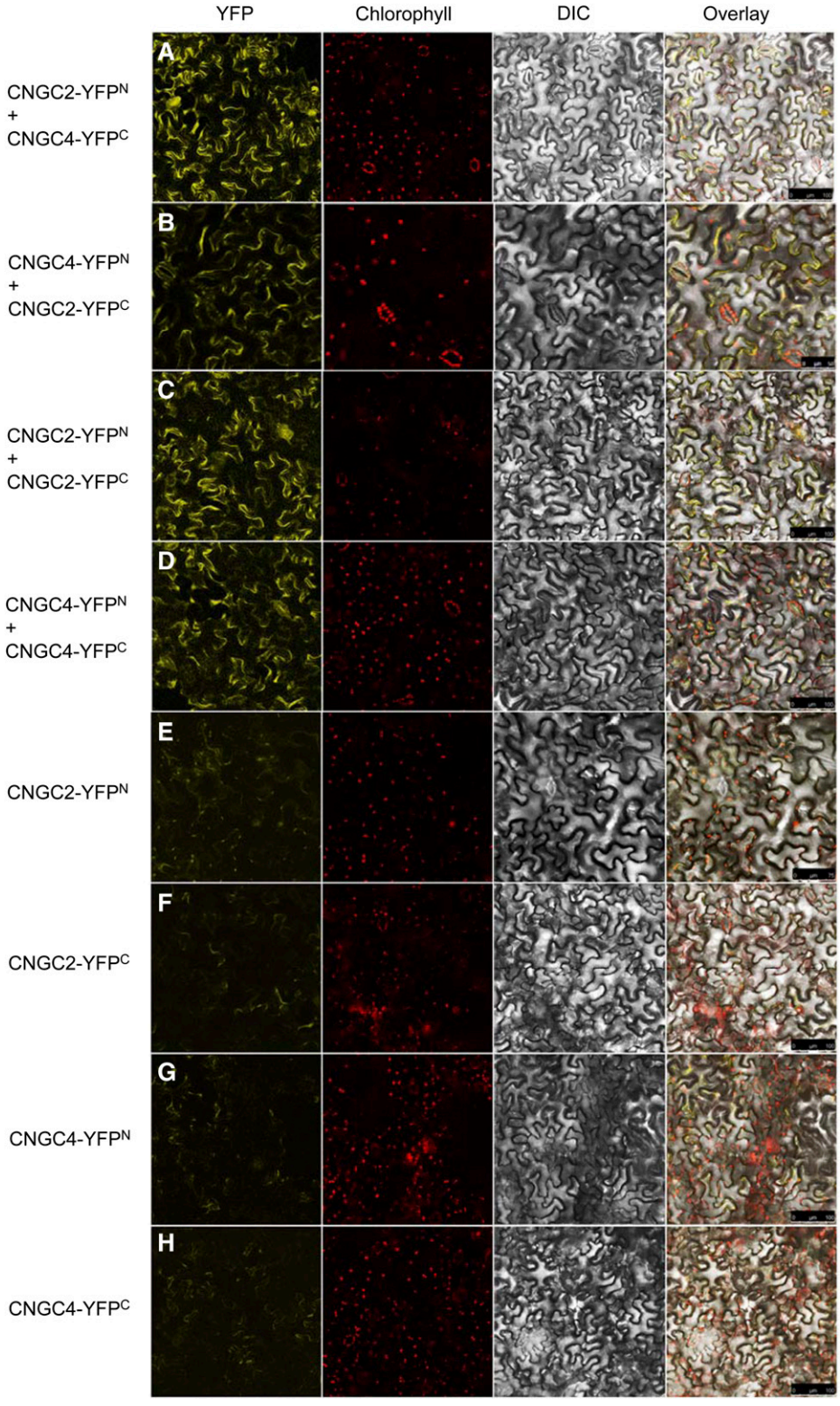

Figure 6. AtCNGC2 and AtCNGC4 subunits interact in planta. BiFC was performed with full-length AtCNGC2 and AtCNGC4 C-terminally fused to the N- and C-terminal portions of YFP (YFP^N and YFP^C respectively). Coexpression of AtCNGC2-YFP^N and AtCNGC4-YFP^C (A), AtCNGC4-YFP^N and AtCNGC2-YFP^C (B), AtCNGC2-YFP^N and AtCNGC2-YFP^C (C), and AtCNGC4-YFP^N and AtCNGC4-YFP^C (D) show reproducible YFP fluorescence. Single expression of each construct served as negative controls (E–H). For additional controls, see Supplemental Figure S7. The columns show YFP fluorescence (left), chlorophyll autofluorescence (middle left), differential interference contrast (DIC; middle right), and an overlay of all three images (right). Bars = 100 μm. [See online article for color version of this figure.]

cilia of olfactory sensory neurons consist of three different subunits, A2, A4, and B1b. Thus, it is generally believed that CNGCs form heterotetrameric complexes consisting of distinct subunits in order to create specific channels (Kaupp and Seifert, 2002).

Plant CNGCs, on the other hand, have only been investigated much more recently. Based on animal CNGC research, plant CNGCs are also suggested to form tetrameric channels. Functional complementation assays in heterologous expression systems, such as

Saccharomyces cerevisiae and *Escherichia coli*, as well as electrophysiological analysis in *Xenopus laevis* oocytes and human embryonic kidney cells indicated that some subunits are also able to form functional homomeric channels (Kaplan et al., 2007; Chin et al., 2009). However, the nature of the subunit composition of CNGCs (i.e. homotetramer or heterotetramer formation in planta) has not yet been revealed.

In this study, in order to understand the CNGC-mediated signal transduction in plant defense responses, we conducted a suppressor screen using the Arabidopsis *dnd1* mutant, which is a null mutant of *AtCNGC2*. Prior to this study, our group conducted a similar suppressor screen using the *cpr22* mutant that resulted from the fusion of *AtCNGC11* and *AtCNGC12* (Yoshioka et al., 2006). This mutant shows similar autoimmune phenotypes to *dnd1*. The suppressor screen using *cpr22*, however, has so far yielded only intragenic mutants and, thus, has not yet revealed novel CNGC-mediated signaling components (Baxter et al., 2008; Chin et al., 2010, Abdel-Hamid et al., 2013). This is mainly due to the gain-of-function nature of *cpr22*. On the other hand, *dnd1* is a loss-of-function mutant, thus making the likelihood of obtaining intragenic mutants very low. Furthermore, we have used a T-DNA insertion line to further increase the probability of obtaining intergenic mutants. This led us to successfully isolate what is, to our knowledge, the first *dnd1* suppressor, *rdd1*, that is described in this study.

AtCNGC2 has been relatively well studied among the Arabidopsis CNGCs and has been reported to be involved in pathogen defense responses. Since *dnd1* has a reduced HR upon pathogen infection, *AtCNGC2* has been proposed to be a positive regulator of defense responses. This notion was demonstrated by Ali et al. (2007), who showed that AtCNGC2 mediates pathogen-associated molecular pattern-triggered activation of defense responses through a cAMP-stimulated Ca^{2+} influx, which leads to increased nitric oxide production. Additionally, they indicated that AtCNGC2-mediated nitric oxide production is also required for *R* gene-mediated HR development. At the same time, *dnd1* is known to exhibit typical autoimmune phenotypes, such as elevated levels of SA, constitutive expression of *PR* genes, and conditional HR-like spontaneous lesion formation without pathogen infection (Yu et al., 1998; Clough et al., 2000). Thus, the precise role of *AtCNGC2* in defense responses is still elusive. Nevertheless, the *rdd1-1D* mutation partially suppressed all of these *dnd1*-mediated phenotypes except Ca^{2+} hypersensitivity. It has been shown that the alteration of HR phenotypes upon pathogen infection is independent from SA accumulation and enhanced resistance in *dnd1* (Clough et al., 2000; Genger et al., 2008). Collectively, these observations suggest that the effect of the *rdd1* mutation occurs relatively upstream in *dnd1*-mediated signaling (i.e. upstream in the signaling pathway) before it branches out to cause the pleiotropic phenotypes of *dnd1* (i.e. loss of HR and SA-dependent enhanced pathogen resistance responses) but after the signal for Ca^{2+} sensitivity branches out. Positional cloning strategies have so far mapped *RDD1* to a region containing approximately 200 genes at the upper arm of chromosome 5 (initial linkage analysis data are presented in Supplemental Fig. S8; Supplemental Table S2). This region does not contain any genes known to suppress CNGC-mediated resistance (Yoshioka et al., 2006; Genger et al., 2008; K. Chin and K. Yoshioka, unpublished data) and also does not contain CNGC2 or CNGC4. Thus *RDD1* is likely a novel component in the CNGC-mediated pathogen resistance signaling pathway itself or in an alternative pathway that can affect the *dnd1* phenotypes.

In addition, two significant findings were made in this study: (1) the involvement of AtCNGC2 in flowering timing, and (2) the possibility that AtCNGC2 and AtCNGC4 form heterotetramers. Recently, several reports connecting pathogen defense and flowering timing have been published (Martínez et al., 2004; Palma et al., 2010; Tsuchiya and Eulgem, 2010; Wang et al., 2011; Li et al., 2012; Quesada et al., 2013). Under normal conditions, flowering timing is tightly regulated by signaling networks that integrate endogenous and external cues to follow seasonal changes (Davis, 2009). However, particular environmental stress conditions, such as UV-C radiation, pathogen infection, and extreme temperatures, can promote flowering (Raskin, 1992). Martínez et al. (2004) have reported that SA positively regulates flowering timing in Arabidopsis. SA was suggested to act as a negative regulator of the central floral repressor, *FLC*, in a photoperiod-dependent manner, as SA-deficient mutants, such as *nahG*, *sid2*, and *eds5/sid1*, exhibit late-flowering phenotypes and increased levels of *FLC* transcript under short-day conditions (Martínez et al., 2004). Consistent with this observation, defense mutants with elevated SA levels, such as *pub13* or *siz1*, display earlier SA-dependent flowering phenotypes (Jin et al., 2008; Li et al., 2012). In our study, however, *dnd1* shows delayed-flowering phenotypes in spite of elevated levels of SA, and this phenotype was observed under both long- and short-day conditions, although it is enhanced in the latter condition. Thus, it is opposite to what was observed by Martínez et al. (2004) as well as for *pub13* or *siz1*. These observations, together with our preliminary analysis using *dnd1/sid2* double mutants, indicate that SA is unlikely to be the cause of the alteration in flowering timing in *dnd1* (K. Chin and K. Yoshioka unpublished data). Interestingly, the Arabidopsis lesion-mimic mutant *rugosa1* (*rug1*) showed a delayed-flowering phenotype with enhanced disease resistance responses, such as accumulation of hydrogen peroxide and elevation of *PR-1* and the SA biosynthetic gene *SID2*, which is reminiscent of *dnd1* (Quesada et al., 2013). *rug1* is a loss-of-function mutant of porphobilinogen deaminase, which is a tetrapyrrole biosynthetic enzyme. The precise molecular mechanisms of *rug1* that induce delayed flowering and autoimmune phenotypes much like *dnd1*, however, are currently unclear. Autoimmune mutants, like *rug1* and *dnd1*, typically show severe developmental defects, and some phenotypes could be attributable to indirect effects of physiological

perturbations. However, a clear cross talk between defense and floral transition has been reported in several cases. For instance, the Arabidopsis mutant *enhanced downy mildew2* (*edm2*) is compromised in disease resistance mediated by the *R* gene *RPP7*. However, the role of *EDM2* in defense is rather limited, and its role in flowering in a *FLC*-dependent manner was reported (Tsuchiya and Eulgem, 2010). EDM2 physically interacts with, and is phosphorylated by, the protein kinase WNK8, which is known to affect the photoperiodic pathways in the floral transition (Wang et al., 2008). Thus, this example provides convincing evidence of the cross talk between defense responses and flowering time. Further analysis of the floral transition in *dnd1* is in progress.

Another significant finding is the relationship between the downstream signaling pathways mediated by AtCNGC2 and AtCNGC4. As shown, *rdd1-1D* not only suppresses *cngc2*-mediated, but also *cngc4*-conferred, phenotypes. Both *hlm1* and *dnd2* are loss-of-function mutants of *AtCNGC4*, which is the closest paralog of *AtCNGC2* and the only other member of group IVB in the AtCNGC family (Mäser et al., 2001). These *cngc4* mutants display almost identical phenotypes to those seen in *cngc2* mutants (Balagué et al., 2003; Genger et al., 2008; Fig. 5). Furthermore, the aforementioned delayed-flowering phenotype is also found in *cngc4* (Supplemental Fig. S5). Therefore, the relationship between these two CNGCs is of interest, and it could be hypothesized that they are both part of the same heterotetrameric channel. However, it has been reported that the loss of both *AtCNGC2* and *AtCNGC4* shows synergistic effects, as *dnd1/dnd2* double mutants display enhanced *dnd* phenotypes (termed *superdnd* in Table II; Supplemental Fig. S3; Jurkowski et al., 2004). This suggests the existence of homotetramers or parallel signaling pathways mediated by AtCNGC2 and AtCNGC4.

In this study, our data showing the suppression of both mutant phenotypes by *rdd1-1D* provides compelling genetic evidence that AtCNGC2- and AtCNGC4-mediated signal transduction pathways are at least overlapping or merge at some point. In addition, our BiFC data indicate in planta interactions between these two subunits as well as with themselves, suggesting the existence of both homotetramers and heterotetramers in planta.

Together with prior data showing the enhancement of the phenotypes in the double mutant (Supplemental Fig. S3; Jurkowski et al., 2004), we propose that AtCNGC2 and AtCNGC4 form heterotetrameric as well as homotetrameric channels in planta and that they share the same biological function. At this moment, it is not known whether both types of channels exist in wild-type plants, but in the single *dnd1* mutant, only AtCNGC4 homotetrameric channels likely could be formed. This would also be the case for *hlm1/dnd2*, which could have only AtCNGC2 homotetramers (Fig. 7, A and B). In the case that wild-type plants have both homotetrameric and heterotetrameric channels (Fig. 7A), they would have at least three different channels with these two subunits, AtCNGC2 homotetrameric, AtCNGC4 homotetrameric, and AtCNGC2 and AtCNGC4 heterotetrameric channels, and they would work synergistically. In this scenario, single mutants would have lost two of the three different channels and, consequently, display the reported phenotypes. Alternatively, the homotetrameric versions may not exist in wild-type plants, possibly due to a lower affinity of homotetramerization compared with heterotetramerization (Fig. 7B). Only when one of the subunits does not exist (i.e. single mutants) would

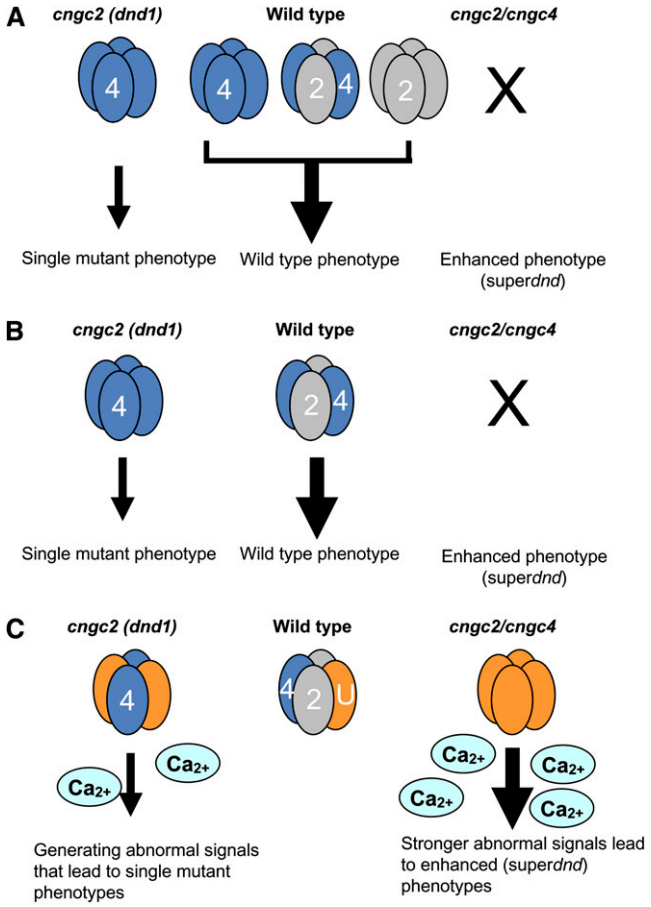

Figure 7. Proposed CNGC compositions involving AtCNGC2 and AtCNGC4 subunits. A, When wild-type plants have three different channels with these two subunits, AtCNGC2 homotetrameric, AtCNGC4 homotetrameric, and AtCNGC2 and four heterotetrameric channels, and they work synergistically. In this scenario, single mutants would have lost two of the three different channels and consequently display the reported phenotypes. B, When wild-type plants have only heterotetrameric channels, single mutants have abnormal homotetrameric channels. In this case, although the function of homotetrameric and heterotetrameric channels may be the same, the efficacy could be different, since double mutants have an enhanced phenotype. C, When unidentified subunit(s) is/are involved to form a channel complex with AtCNGC2 and AtCNGC4 in wild-type plants. In this case, the absence of AtCNGC2, AtCNGC4, or both may create an aberrant channel that would lead to an uncontrolled influx of Ca^{2+} into the cell. Unidentified subunit (U) is functionally redundant, since no *dnd*-like phenotype has so far been observed in other AtCNGC knockout mutants. [See online article for color version of this figure.]

homotetrameric channels form abnormally. This is possible, since stronger BiFC signals were observed in two out of three experiments when we coexpressed *AtCNGC2* and *AtCNGC4* compared with single-gene expression (data not shown). In this case, although the function of homotetrameric and heterotetrameric channels might be the same, the efficacy could be different (i.e. heterotetrameric channels may function more effectively than homotetrameric ones). This could lead to the reported phenotypes in *cngc2* and *cngc4* mutants and the enhanced *dnd* phenotype in the double mutant (Jurkowski et al., 2004). This model can explain our observations as well as previously reported data. Another possibility that cannot be excluded is that AtCNGC2 and AtCNGC4 form a channel with an additional unidentified subunit(s). In this case, the absence of AtCNGC2, AtCNGC4, or both may create an increasingly aberrant channel that would lead to an uncontrolled influx of Ca^{2+} into the cell (Fig. 7C). This model would explain the increased cytosolic [Ca^{2+}] levels in *cngc2* plants (Chan et al., 2008; see below). A similar idea was discussed by Tunc-Ozdemir et al. (2013). Thus, further studies regarding the subunit composition of CNGCs are required.

The precise mechanisms by which the lack of these CNGCs can induce autoimmunity, delayed flowering, and hypersensitivity to Ca^{2+} under normal conditions without specific stimulations are still elusive, but they can be explained by their housekeeping roles to maintain stable physiology in plant cells. Recently, Finka et al. (2012) reported that *AtCNGC2* and its *Physcomitrella patens* ortholog, CNGCb, act as the primary thermosensors of land plant cells. Interestingly, CNGCb loss of function caused a hyperthermoresponsive Ca^{2+} influx and a systemic higher background of cytosolic [Ca^{2+}]. A similar observation was made by Chan et al. (2008), who demonstrated that *cngc2* plants displayed a gene expression profile similar to that of wild-type plants grown in high external Ca^{2+}. Such abnormally high levels of Ca^{2+} ions could cause the alterations in defense and developmental signal transduction that are observed in *dnd1* and *hlm1/dnd2*. In addition, CNGCs may have multiple biological functions, as *AtCNGC11* and *AtCNGC12* have been reported to mediate multiple Ca^{2+}-dependent physiological responses (Urquhart et al., 2011). *AtCNGC2* has previously been shown to play an additional role in senescence (Köhler et al., 2001; Ma et al., 2010). To further understand the role of plant CNGCs, the identification of more downstream signaling components is required. Thus, the identity of *RDD1* and its involvement in CNGC2- and CNGC4-mediated phenotypes will provide new insight to this aspect. The cloning of *RDD1* is currently in progress.

MATERIALS AND METHODS

Plant Materials and Growth Conditions

The null mutant for Arabidopsis (*Arabidopsis thaliana*) *AtCNGC2*, *dnd1*, was originally identified by Yu et al. (1998) and then was called *dnd1-1* by Genger et al. (2008) and *cngc2-1* by Chan et al. (2003). We use the original name *dnd1* in this paper. Another allele, *cngc2-2*, was also reported (Chan et al., 2003); thus, we named our T-DNA insertion line (Salk_066908) *cngc2-3*. The allelic null mutants for *AtCNGC4* have been reported by Balagué et al. (2003) as *hlm1-1*, *hlm1-2*, and *hlm1-3* and as *dnd2-1* by Jurkowski et al. (2004). We used *dnd2-1* from Jurkowski et al. (2004) in this paper and used the name *dnd2* to avoid confusion. The T-DNA insertion knockout line for AtCNGC4 that was used in this study (Salk_081369) thus was named *cngc4-5*. The seeds were planted on Sunshine Mix 1 (Sun Gro Horticulture Canada) and stratified at 4°C for 4 d. Plants were either grown in a growth chamber with a 9-h photoperiod (9 h of light/15 h of dark) and a day/night temperature regime of 22°C/18°C or a 16-h photoperiod (16 h of light/8 h of dark) at 22°C.

Suppressor Screening and Identification of *rdd1*

Approximately 10,000 *cngc2* T-DNA (Salk_066908) mutant seeds were mutagenized with 0.3% (v/v) ethyl methanesulfonate solution (Sigma-Aldrich) for 8 h, followed by rinsing more than 15 times in water. These M0 seeds were grown under ambient humidity for M1 plants. The M2 seeds were collected and then screened for mutants suppressing the dwarf phenotype conferred by the *cngc2* mutation. *rdd1-1D cngc2-3* was identified based on its intermediate morphology between Col wild-type and *cngc2-3* plants. It was backcrossed twice with a homozygous *cngc2-3* plant for genetic analysis.

Pathogen Infection Assays

Bacterial infection was conducted as reported previously (Yoshioka et al., 2006) using 5- to 6-week-old plants. Infection with *Hyaloperonospora arabidopsidis*, isolate Noco2, was performed as described previously with 8×10^5 spores mL^{-1} (Yoshioka et al., 2006).

Ca^{2+} Sensitivity Assay

Wild-type and mutant plants were grown on 0.5× Murishage and Skoog salt, 2.5 mM MES, 1% (v/w) Suc, and 0.8% agar, pH 5.7. Calcium sensitivity was tested on Murishage and Skoog medium supplemented with 5, 10, and 20 mM $CaCl_2$. All plants were grown under continuous light.

RNA Extraction and qRT-PCR

Small-scale RNA extraction was carried out using the TRIzol reagent (Invitrogen) according to the manufacturer's instructions. qRT-PCR was performed as described previously (Mosher et al., 2010) using *ELONGATION FACTOR-1α (EF-1α)* gene expression for normalization. Primer sequences are listed in Supplemental Table S2.

Extraction and Analysis of SA

Endogenous SA was analyzed as described previously (Mosher et al., 2010).

BiFC and *Agrobacterium tumefaciens* Infiltration

For BiFC analysis, full-length *AtCNGC2* and *AtCNGC4* complementary DNAs were subcloned into the Gateway entry vector pDONR221 (Invitrogen; http://www.invitrogen.com). Subsequently, all clones were subcloned into the destination vectors for plant expression, pK2GWYn9 (nYFP), pL2GWYc9 (cYFP), or pEARLEY101 (full-length YFP, controlled by the cauliflower mosaic virus 35S promoter; Earley et al., 2006) using LR Clonase (Invitrogen; http://www.invitrogen.com) according to the manufacturer's instructions. All constructed plasmids were sequenced for fidelity.

Constructs were then transformed into *A. tumefaciens* strain GV2260. Individual colonies were grown for 20 h at 30°C in Luria-Bertani medium and then subcultured into medium 1 (Luria-Bertani medium, 10 mM MES, and 20 μM acetosyringone) for 20 h. Cultures were then washed in infiltration medium (10 mM $MgCl_2$, 10 mM MES, and 150 μM acetosyringone) and resuspended to an optical density at 600 nm of 0.5. Cultures were incubated overnight at room temperature and syringe infiltrated into 6-week-old *Nicotiana benthamiana* leaves. N- and C- terminal YFP fusions were coinfiltrated with HC-Pro of *Tobacco etch virus*. Leaf discs of infiltrated areas were excised 48 h after inoculation and used for confocal microscopy.

Microscopy

HR-associated autofluorescence was monitored using the fluorescein isothiocyanate/GFP filter on the Leica DMI3000 inverted microscope. Confocal fluorescence images were acquired using a Leica TCS SP5 confocal system with the acousto-optical beam splitter (HCX PL APO CS 40x immersion oil objective; numerical aperture, 1.25) with the acousto-optic tunable filter for the argon laser set at 20% and the detection window at 525 to 600 nm for YFP (Leica Microsystems). Autofluorescence of chloroplasts was detected at 650 to 700 nm.

Sequence data from this article can be found in the GenBank/EMBL data libraries under accession numbers DND1 (CNGC2), AT5G15410, DND2/HLM1 (CNGC4), and AT5G54250.

Supplemental Data

The following materials are available in the online version of this article.

Supplemental Figure S1. Analysis of T-DNA insertion lines and confirmation of the status of rdd1-1D cngc2-3.

Supplemental Figure S2. rdd1-1D does not rescue Ca^{2+} hypersensitivity in cngc2.

Supplemental Figure S3. Analysis of rdd1-1D cngc4-5, rdd1-1D cngc2-3 cngc4-5, and superdnd (cngc2-3 cngc4-5).

Supplemental Figure S4. The rdd1-1D single mutant does not display the rdd1-1D cngc2-3 phenotype.

Supplemental Figure S5. rdd1-1D represses cngc4- and dnd2-mediated delay in floral transition.

Supplemental Figure S6. FPLC analysis of GST-2Ct and MBP-4Ct proteins.

Supplemental Figure S7. Coexpression of AtCNGC4 and AtCNGC2 with AtCNGC11/12 shows no YFP fluorescence.

Supplemental Figure S8. Marker used for linkage mapping.

Supplemental Table S1. Flowering time under short day condition.

Supplemental Table S2. Genetic linkage analysis of *rdd1/cngc2-1* Wassilewskija F2 generation.

Supplemental Table S3. Primers used in this study.

Supplemental Materials and Methods S1. Recombinant protein expression, purification, and FPLC analysis.

ACKNOWLEDGMENTS

We thank Dr. Andrew Bent and Dr. Catherine W.M. Chan for providing the seeds of various double mutants of *dnd1* and *dnd2* and *cngc2-2*, respectively. We also thank Nicole Cho, Jihyun Lee, Brenden A. Hurley and Alex Fortuna for their assistance.

Received July 26, 2013; accepted September 11, 2013; published September 11, 2013.

LITERATURE CITED

Abdel-Hamid H, Chin K, Moeder W, Shahinas D, Gupta D, Yoshioka K (2013) A suppressor screen of the chimeric *AtCNGC11/12* reveals residues important for intersubunit interactions of cyclic nucleotide-gated ion channels. Plant Physiol **162:** 1681–1693

Ali R, Ma W, Lemtiri-Chlieh F, Tsaltas D, Leng Q, von Bodman S, Berkowitz GA (2007) Death don't have no mercy and neither does calcium: *Arabidopsis* CYCLIC NUCLEOTIDE GATED CHANNEL2 and innate immunity. Plant Cell **19:** 1081–1095

Balagué C, Lin B, Alcon C, Flottes G, Malmström S, Köhler C, Neuhaus G, Pelletier G, Gaymard F, Roby D (2003) HLM1, an essential signaling component in the hypersensitive response, is a member of the cyclic nucleotide-gated channel ion channel family. Plant Cell **15:** 365–379

Baxter J, Moeder W, Urquhart W, Shahinas D, Chin K, Christendat D, Kang HG, Angelova M, Kato N, Yoshioka K (2008) Identification of a functionally essential amino acid for Arabidopsis cyclic nucleotide gated ion channels using the chimeric *AtCNGC11/12* gene. Plant J **56:** 457–469

Chan CWM, Schorrak LM, Smith RK Jr, Bent AF, Sussman MR (2003) A cyclic nucleotide-gated ion channel, CNGC2, is crucial for plant development and adaptation to calcium stress. Plant Physiol **132:** 728–731

Chan CWM, Wohlbach DJ, Rodesch MJ, Sussman MR (2008) Transcriptional changes in response to growth of *Arabidopsis* in high external calcium. FEBS Lett **582:** 967–976

Chin K, Moeder W, Abdel-Hamid H, Shahinas D, Gupta D, Yoshioka K (2010) Importance of the alphaC-helix in the cyclic nucleotide binding domain for the stable channel regulation and function of cyclic nucleotide gated ion channels in Arabidopsis. J Exp Bot **61:** 2383–2393

Chin K, Moeder W, Yoshioka K (2009) Biological roles of cyclic-nucleotide-gated ion channels in plants: what we know and don't know about this 20 member ion channel family. Botany **87:** 668–677

Clough SJ, Fengler KA, Yu IC, Lippok B, Smith RK Jr, Bent AF (2000) The Arabidopsis dnd1 "defense, no death" gene encodes a mutated cyclic nucleotide-gated ion channel. Proc Natl Acad Sci USA **97:** 9323–9328

Craven KB, Zagotta WN (2006) CNG and HCN channels: two peas, one pod. Annu Rev Physiol **68:** 375–401

Davis SJ (2009) Integrating hormones into the floral-transition pathway of Arabidopsis thaliana. Plant Cell Environ **32:** 1201–1210

Earley KW, Haag JR, Pontes O, Opper K, Juehne T, Song K, Pikaard CS (2006) Gateway-compatible vectors for plant functional genomics and proteomics. Plant J **45:** 616–629

Finka A, Cuendet AF, Maathuis FJ, Saidi Y, Goloubinoff P (2012) Plasma membrane cyclic nucleotide gated calcium channels control land plant thermal sensing and acquired thermotolerance. Plant Cell **24:** 3333–3348

Frietsch S, Wang YF, Sladek C, Poulsen LR, Romanowsky SM, Schroeder JI, Harper JF (2007) A cyclic nucleotide-gated channel is essential for polarized tip growth of pollen. Proc Natl Acad Sci USA **104:** 14531–14536

Genger RK, Jurkowski GI, McDowell JM, Lu H, Jung HW, Greenberg JT, Bent AF (2008) Signaling pathways that regulate the enhanced disease resistance of Arabidopsis "defense, no death" mutants. Mol Plant Microbe Interact **21:** 1285–1296

Greenberg JT, Yao N (2004) The role and regulation of programmed cell death in plant-pathogen interactions. Cell Microbiol **6:** 201–211

Hammond-Kosack KE, Jones JDG (1996) Resistance gene-dependent plant defense responses. Plant Cell **8:** 1773–1791

He Y, Amasino RM (2005) Role of chromatin modification in flowering-time control. Trends Plant Sci **10:** 30–35

Jin JB, Jin YH, Lee J, Miura K, Yoo CY, Kim WY, Van Oosten M, Hyun Y, Somers DE, Lee I, et al (2008) The SUMO E3 ligase, AtSIZ1, regulates flowering by controlling a salicylic acid-mediated floral promotion pathway and through affects on FLC chromatin structure. Plant J **53:** 530–540

Jirage D, Zhou N, Cooper B, Clarke JD, Dong X, Glazebrook J (2001) Constitutive salicylic acid-dependent signaling in cpr1 and cpr6 mutants requires PAD4. Plant J **26:** 395–407

Jurkowski GI, Smith RK Jr, Yu IC, Ham JH, Sharma SB, Klessig DF, Fengler KA, Bent AF (2004) Arabidopsis DND2, a second cyclic nucleotide-gated ion channel gene for which mutation causes the "defense, no death" phenotype. Mol Plant Microbe Interact **17:** 511–520

Kaplan B, Sherman T, Fromm H (2007) Cyclic nucleotide-gated channels in plants. FEBS Lett **581:** 2237–2246

Kaupp UB, Seifert R (2002) Cyclic nucleotide-gated ion channels. Physiol Rev **82:** 769–824

Köhler C, Merkle T, Roby D, Neuhaus G (2001) Developmentally regulated expression of a cyclic nucleotide-gated ion channel from Arabidopsis indicates its involvement in programmed cell death. Planta **213:** 327–332

Leng Q, Mercier RW, Hua BG, Fromm H, Berkowitz GA (2002) Electrophysiological analysis of cloned cyclic nucleotide-gated ion channels. Plant Physiol **128:** 400–410

Leng Q, Mercier RW, Yao W, Berkowitz GA (1999) Cloning and first functional characterization of a plant cyclic nucleotide-gated cation channel. Plant Physiol **121:** 753–761

Li W, Ahn IP, Ning Y, Park CH, Zeng L, Whitehill JG, Lu H, Zhao Q, Ding B, Xie Q, et al (2012) The U-box/ARM E3 ligase PUB13 regulates cell death, defense, and flowering time in Arabidopsis. Plant Physiol **159:** 239–250

Ma W, Smigel A, Walker RK, Moeder W, Yoshioka K, Berkowitz GA (2010) Leaf senescence signaling: the Ca^{2+}-conducting Arabidopsis cyclic

nucleotide gated channel2 acts through nitric oxide to repress senescence programming. Plant Physiol **154:** 733–743

Martínez C, Pons E, Prats G, León J (2004) Salicylic acid regulates flowering time and links defence responses and reproductive development. Plant J **37:** 209–217

Mäser P, Thomine S, Schroeder JI, Ward JM, Hirschi K, Sze H, Talke IN, Amtmann A, Maathuis FJ, Sanders D, et al (2001) Phylogenetic relationships within cation transporter families of Arabidopsis. Plant Physiol **126:** 1646–1667

McAinsh MR, Schroeder JI (2009) Crosstalk in Ca^{2+} signaling pathways. *In* K Yoshioka, K Shinozaki, eds, Signal Crosstalk in Plant Stress Response. Wiley-Blackwell, Hoboken, NJ, pp 59–95

Moeder W, Urquhart W, Ung H, Yoshioka K (2011) The role of cyclic nucleotide-gated ion channels in plant immunity. Mol Plant **4:** 442–452

Mosher S, Moeder W, Nishimura N, Jikumaru Y, Joo S-H, Urquhart W, Klessig DF, Kim SK, Nambara E, Yoshioka K (2010) The lesion-mimic mutant *cpr22* shows alterations in abscisic acid signaling and abscisic acid insensitivity in a salicylic acid-dependent manner. Plant Physiol **152:** 1901–1913

Palma K, Thorgrimsen S, Malinovsky FG, Fiil BK, Nielsen HB, Brodersen P, Hofius D, Petersen M, Mundy J (2010) Autoimmunity in Arabidopsis acd11 is mediated by epigenetic regulation of an immune receptor. PLoS Pathog **6:** e1001137

Quesada V, Sarmiento-Mañús R, González-Bayón R, Hricová A, Ponce MR, Micol JL (2013) PORPHOBILINOGEN DEAMINASE deficiency alters vegetative and reproductive development and causes lesions in Arabidopsis. PLoS ONE **8:** e53378

Raskin I (1992) Role of salicylic acid in plants. Annu Rev Plant Physiol Plant Mol Biol **43:** 439–463

Spalding EP, Harper JF (2011) The ins and outs of cellular Ca^{2+} transport. Curr Opin Plant Biol **14:** 715–720

Talke IN, Blaudez D, Maathuis FJM, Sanders D (2003) CNGCs: prime targets of plant cyclic nucleotide signalling? Trends Plant Sci **8:** 286–293

Tsuchiya T, Eulgem T (2010) The Arabidopsis defense component EDM2 affects the floral transition in an FLC-dependent manner. Plant J **62:** 518–528

Tunc-Ozdemir M, Tang C, Ishka MR, Brown E, Groves NR, Myers CT, Rato C, Poulsen LR, McDowell S, Miller G, et al (2013) A cyclic nucleotide-gated channel (CNGC16) in pollen is critical for stress tolerance in pollen reproductive development. Plant Physiol **161:** 1010–1020

Urquhart W, Chin K, Ung H, Moeder W, Yoshioka K (2011) The cyclic nucleotide-gated channels AtCNGC11 and 12 are involved in multiple Ca^{2+}-dependent physiological responses and act in a synergistic manner. J Exp Bot **62:** 3671–3682

Urquhart W, Gunawardena AHLAN, Moeder W, Ali R, Berkowitz GA, Yoshioka K (2007) The chimeric cyclic nucleotide-gated ion channel ATCNGC11/12 constitutively induces programmed cell death in a Ca^{2+} dependent manner. Plant Mol Biol **65:** 747–761

Wang GF, Seabolt S, Hamdoun S, Ng G, Park J, Lu H (2011) Multiple roles of WIN3 in regulating disease resistance, cell death, and flowering time in Arabidopsis. Plant Physiol **156:** 1508–1519

Wang Y, Liu K, Liao H, Zhuang C, Ma H, Yan X (2008) The plant WNK gene family and regulation of flowering time in Arabidopsis. Plant Biol (Stuttg) **10:** 548–562

Yoshioka K, Kachroo P, Tsui F, Sharma SB, Shah J, Klessig DF (2001) Environmentally sensitive, SA-dependent defense responses in the cpr22 mutant of Arabidopsis. Plant J **26:** 447–459

Yoshioka K, Moeder W, Kang HG, Kachroo P, Masmoudi K, Berkowitz G, Klessig DF (2006) The chimeric *Arabidopsis* CYCLIC NUCLEOTIDE-GATED ION CHANNEL11/12 activates multiple pathogen resistance responses. Plant Cell **18:** 747–763

Yu IC, Parker J, Bent AF (1998) Gene-for-gene disease resistance without the hypersensitive response in Arabidopsis dnd1 mutant. Proc Natl Acad Sci USA **95:** 7819–7824

Zagotta WN, Siegelbaum SA (1996) Structure and function of cyclic nucleotide-gated channels. Annu Rev Neurosci **19:** 235–263

Zufall F, Firestein S, Shepherd GM (1994) Cyclic nucleotide-gated ion channels and sensory transduction in olfactory receptor neurons. Annu Rev Biophys Biomol Struct **23:** 577–607